

Article ID: 1007-4627(2018)04-0420-09

# Competition Between the Single-particle Seniority Regime and Collective Motion in Intermediate-mass Nuclei

QI Chong

(KTH Royal Institute of Technology, SE-10691 Stockholm, Sweden)

**Abstract:** The E2 transition strength,  $B(E2)$ , gives particularly precise information on the competition between the collective and single-particle degree of freedom. An important observable to study the development of collectivity is the  $B(E2; 4_1^+ \rightarrow 2_1^+)/B(E2; 2_1^+ \rightarrow g.s.)$  ( $B_{4/2}$ ). The  $B_{4/2}$  ratio is usually greater than unity. These values are 1.4 and 2.0 for an ideal rotor and a vibrator, respectively. Whereas the seniority scheme usually leads to different behaviours. In this contribution I will show examples that contrast with our standard understanding. The yrast spectra of Te isotopes show a vibrational-like equally-spaced pattern but the few known E2 transitions show anomalous rotational-like behaviour, which cannot be reproduced by collective models. Large-scale shell model calculations reproduce well the equally-spaced spectra of those isotopes as well as the constant behaviour of the  $B(E2)$  values in  $^{114}\text{Te}$ . For nuclei involving protons or neutrons in  $j=9/2$  orbitals, the partial conservation of seniority can lead to dramatic changes to the E2 decay pattern that have never been seen before. The  $B_{4/2}$  ratios in quantum phase transitional nuclei around  $N=90$  also show a similar exotic feature.

**Key words:** electromagnetic transition; shell model; seniority; collectivity

**CLC number:** O571.6; P142.9      **Document code:** A      **DOI:** 10.11804/NuclPhysRev.35.04.420

## 1 Introduction

The advent of radioactive ion beam facilities and new detector technologies have opened up new possibilities to investigate the radioactive decays of highly unstable nuclei. Recent investments in new facilities such as FAIR at GSI, Darmstadt, FRIB at MSU and HIAF at HuiZhou will produce unprecedented data on exotic nuclei and nuclear matter that are relevant our understanding of nuclear structure by also for nuclear astrophysical processes. In particular, one fundamental nuclear physics question one aims at addressing is how are complex nuclei built from their basic constituents and how to explain collective phenomena from individual motion? The emergence of collective behaviour outside closed-shell configurations represents one of the most important paradigms in the description of finite atomic nuclei. An emergence of collectivity can be observed even one has only several nucleons away from the neutron and proton magic numbers. The excitation energies and lifetimes of the first excited  $2^+$  and  $4^+$  states in atomic nuclei with even numbers of neutrons and protons are fundamental observables. These quantities constitute key benchmarks for testing and

differentiating between essentially all possible nuclear modes, from the single-particle to the collective regime. The vibrational or rotational degrees of collective freedom is normally associated with a lowering of the first excited  $2^+$  state energy accompanied by an increase in the  $2_1^+ \rightarrow g.s.$  reduced electric quadrupole transition strength,  $B(E2)$ . A gradual evolution of  $B(E2)$  (or  $E(2_1^+)$ ) values is often expected along an isotopic chain: from spherical systems near closed shells and governed by the individual single-particle degrees of freedom where the strength is at a minimum, via quadrupole surface vibrations around spherical symmetry, to the gradual development of deformation with associated strong E2 transitions and to a spherical system again when approaching the next major shell. The maximal  $B(E2)$  values are expected to be seen in the middle between major shell closures.

The  $B(E2)$  values usually increase with spin for low-lying states within a collective (rotational or vibrational) band structure. As a consequence, the  $B(E2; 4_1^+ \rightarrow 2_1^+)/B(E2; 2_1^+ \rightarrow g.s.)$  ratio ( $B_{4/2}$ ) is strictly larger than unity for collective excitations. For an ideal rotor, a value of  $B_{4/2}=10/7=1.43$  is expected (known as the Alaga rule) whereas for a harmonic vi-

**Received date:** 18 Oct. 2018

**Foundation item:** Swedish Research Council (VR) (621-2012-3805, 621-2013-4323) and Göran Gustafsson Foundation.

**Biography:** QI Chong(1983-), Shandong Province, Associate Professor, working on nuclear structure physics;  
E-mail: [chongq@kth.se](mailto:chongq@kth.se); [chong.kth@gmail.com](mailto:chong.kth@gmail.com).

brator one has  $B_{4/2}=2$ , reflecting the ratio between the number of phonons in the involved states. The ratio can be smaller than one in structures exhibiting seniority symmetry near neutron and/or proton magic numbers. It may also be expected to be small in shape-coexisting structures if there is small overlap between the initial and final state. But so far that feature has not been observed. A handful of anomalous cases with  $B_{4/2} < 1$  has been observed in the entire Segre chart<sup>[1-2]</sup>.

In this contribution I would like to discuss briefly structure studies of intermediate-mass and heavy nuclei in relation to  $B_{4/2}$  and the application of the so-called large-scale configuration interaction shell model approach in explaining those features. I will first give a brief review on the challenges and recent developments of the nuclear shell model approach in our group. I will then show some results we obtained recently for intermediate-mass and heavy nuclei around <sup>100</sup>Sn and  $N=90$ . I will explain the structure and decay studies of those nuclei, regarding both experimental and theoretical opportunities.

## 2 Configuration interaction shell model approach

Nuclear structure theory plays an important role in explaining the regular emerging phenomena in nuclear many-body systems. The so-called *ab initio* approaches (in the sense that realistic nucleon-nucleon interaction is applied without significant *ad hoc* adjustment), the nuclear shell model defined in a finite model space and the density functional theory (nuclear mean field) are the most commonly employed microscopic nuclear models nowadays. Those models treat the mean field in quite different ways. The no-core shell model approach aims at considering the residual correlation between all nuclei in a large space defined by the harmonic oscillators. Those studies are constrained to very light nuclei. The modern nuclear shell model (different from the independent particle model) is a full configuration interaction approach. It considers the mixing effect of all possible configurations within a given model space. The model space is usually defined by taking a few single-particle orbitals near the Fermi surface. The number of orbitals one can include is highly restricted due to computation limitation. The nuclear shell model calculation can be actually as challenging as many *ab initio* models from a computational point of view. Extensive studies on algorithm optimization and truncation methods have been carried out. State-of-the-art configuration interaction algorithms can allow us to diagonalize ma-

trices with dimension up to  $2 \times 10^{10}$ . Other challenges of the no core and full configuration interaction shell model approaches include for examples the connection of their effective interaction to fundamental forces like the tensor force and three-body forces, *etc* and the complexity of the their wave function. Despite of these challenges, the nuclear shell model is by far the most accurate and precise theory available on the market.

The residual interaction between valence particles around the Fermi surface is mostly supposed to be of two-body nature. The effective Hamiltonians can be written in terms of single-particle energies and two-body matrix elements as follows (neglecting three-body terms),

$$H_{\text{eff}} = \sum_{\alpha} \varepsilon_{\alpha} \hat{N}_{\alpha} + \frac{1}{4} \sum_{\alpha\beta\delta\gamma JT} \langle \alpha\beta | V | \gamma\delta \rangle_{JT} A_{JT}^{\dagger}; \alpha\beta A_{JT}; \delta\gamma, \quad (1)$$

where we have assumed that the effective Hamiltonian conserves isospin symmetry,  $\alpha = \{nljt\}$  denote the single-particle orbitals and  $\varepsilon_{\alpha}$  stand for the corresponding single-particle energies.  $\hat{N}_{\alpha} = \sum_{j_z, t_z} a_{\alpha, j_z, t_z}^{\dagger} a_{\alpha, j_z, t_z}$  is the particle number operator.  $\langle \alpha\beta | V | \gamma\delta \rangle_{JT}$  are the two-body matrix elements coupled to spin  $J$  and isospin  $T$ .  $A_{JT}$  ( $A_{JT}^{\dagger}$ ) is the fermion pair annihilation (creation) operator.

One may rewrite the Hamiltonian as  $H_{\text{eff}} = H_{\text{m}} + H_{\text{M}}$  where  $H_{\text{m}}$  and  $H_{\text{M}}$  denote the so-called monopole and Multipole Hamiltonians, respectively. The shell model energies can be written as

$$E_i^{\text{SM}} = \sum_{\alpha} \varepsilon_{\alpha} \langle \hat{N}_{\alpha} \rangle + \sum_{\alpha \leq \beta} V_{m; \alpha\beta} \left\langle \frac{\hat{N}_{\alpha}(\hat{N}_{\beta} - \delta_{\alpha\beta})}{1 + \delta_{\alpha\beta}} \right\rangle + \langle \Psi_i | H_{\text{M}} | \Psi_i \rangle, \quad (2)$$

where  $\sum_{\alpha} \langle \hat{N}_{\alpha} \rangle = N$ ,  $\Psi_i$  is the calculated shell-model wave function of the state  $i$ .

The size of the shell-model basis, which quickly goes out of control, can be reduced by apply various truncation approaches. The simplest way of truncation is to restrict the maximal/minimal numbers of particles in different orbitals. This method is applied both to no-core (often being referred to Nmax) and empirical shell model (nphn) calculations. In Ref. [3] we studied the structure and electromagnetic transition properties of light Sn isotopes within the large *gdsh*<sub>11/2</sub> model space by restricting the maximal number of four neutrons that can be excited out of the *g*<sub>9/2</sub> orbital. However, the convergence can be very slow if there is no clear shell or subshell closure or if single-particle structure are significantly modified by

the monopole interaction, as it happens in neutron-rich light nuclei (see, *e.g.*, Ref. [4]).

In addition, one can evaluate the importance of a given basis vector  $\psi_i$  within a partition through a perturbation measure  $R_i = |\langle \psi_i | H_{\text{eff}} | \psi_c \rangle| / (\epsilon_i - \epsilon_c)$  where  $\psi_c$  is the chosen reference with unperturbed energy  $\epsilon_c$ . It is expected that the basis vectors with larger  $R_i$  should play larger role in the given state dominated by the reference basis  $\psi_c$ , from which truncation scheme can be defined. The off-diagonal matrix elements  $\langle \psi_i | H_{\text{eff}} | \psi_c \rangle$  are relatively weak in comparison to the diagonal ones. The most important configurations may be selected by considering the difference of unperturbed energy difference as  $r_i = \epsilon_i - \epsilon_c$ . A truncated model space can thus be defined by taking those with smallest  $r_i$ . The challenge here is that the truncated bases may not conserve angular momentum. An angular momentum conserved correlated basis truncation approach is introduced in Ref. [5]. We are implementing this method in the widely distributed shell-model code NuShellX by replacing its projection sub-routine with our new correlated basis method.

We have also developed an importance truncation based on the total monopole energy as [6]

$$E_P^m = \sum_{\alpha} \varepsilon_{\alpha} N_{P;\alpha} + \sum_{\alpha \leq \beta} V_{m;\alpha\beta} \frac{N_{P;\alpha}(N_{P;\beta} - \delta_{\alpha\beta})}{1 + \delta_{\alpha\beta}}, \quad (3)$$

where  $N_{P;\alpha}$  denotes the particle distributions within a given partition  $P$ . One can order all partitions according to the monopole energy  $E_P^m$  and consider the lowest ones for a given truncation calculation. The idea behind is that the Hamiltonian is dominated by the diagonal monopole channel. The monopole interaction can change significantly the (effective) mean field and drive the evolution of the shell structure. We have done truncation calculations for two isotopes  $^{200,194}\text{Pb}$ . Convergence can be reached with a small portion (around 10%) of the total M-scheme wave function in both cases. This truncation approach can be easily implemented in most existing shell model codes [7].

The two-body matrix elements of the effective Hamiltonian can be calculated from realistic nucleon-nucleon potential where one has to consider the effect of its short range repulsion and the core polarization effects induced by the assumed inert core. However, an optimization of the monopole interaction is necessary in most cases due to the neglect of explicit three-body force and other effects. Shell-model calculations with those optimized interactions have been shown to be very successful in describing nuclei below  $^{100}\text{Sn}$ . Now we aim at giving a microscopic description of heavier nuclei. We have constructed effective interactions for nuclei in the Sn and Pb [6] region. They are the

longest isotopic chains that can be studied by the nuclear shell model and provide excellent ground to study the competition of single-particle and two-body excitations. Our shell-model calculations can reproduce well the binding energies and excitation energies of the low-lying states in those isotopes. A good agreement is also seen for the empirical pairing gaps which can be extracted from the binding energy and can carry important information on the two-nucleon pair clustering as well as  $\alpha$  clustering in the nuclei involved [8–9]. We have been evaluating the structure and decay properties of nuclei around  $N = Z = 50$  and  $Z = 82$  as well as heavier open-shell nuclei within  $gdsh_{11/2}$  shell (see, for examples, Refs. [10–11]).

In Fig. 1 we plotted the M-scheme dimensions for even-even Sn, Te, Xe and Ba isotopes above  $^{100}\text{Sn}$ . We can diagonalize matrices upto dimension  $2 \times 10^{10}$  on the supercomputer Beskow at KTH, Sweden. With the help of that, we have studied systematically all Sn, Sb and Te as well as neutron-deficient Pb isotopes. We have also studied heavier isotopes including  $^{114,128}\text{Xe}$  and  $^{112,132}\text{Ba}$ .

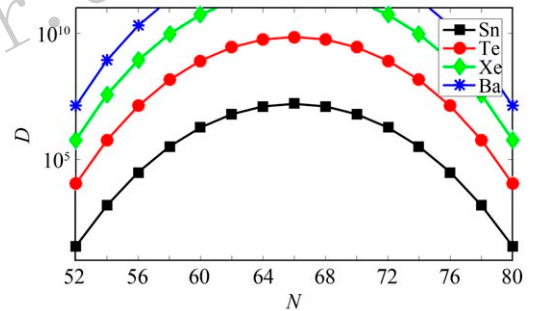


Fig. 1 (color online) Number of  $M^\pi = 0^+$  states in even-even nuclei just above  $^{100}\text{Sn}$ .

### 3 Partial seniority conservation and unusual E2 transition scheme

The seniority quantum number refers to the number of unpaired particles in a single- $j$  shell for a given configuration  $|j^n; I\rangle$  with angular momentum  $I$  [12]. The seniority coupling has shown remarkable success in describing the spectroscopy and electromagnetic transition properties of semi-magic nuclei with spherical symmetry. This is related to the fact that the  $T=1$  two-body matrix elements is dominated by  $J=0$  pairing interactions. Of particular interest are nuclei that can be well approximated by the seniority coupling in high  $j$  orbitals like  $0f_{7/2}$ . Seniority remains a good quantum number within a subshell when  $j \leq 7/2$ . All states in such systems can be uniquely specified by the total angular momentum  $I$  and seniority  $v$ .

The interaction matrix elements have to satisfy a number of constraints in order to conserve seniority

when  $j > 7/2$ . For a subshell with  $j=9/2$ , where all but one two-body matrix elements conserve seniority, the condition reads<sup>[12–17]</sup>

$$65V_2 - 315V_4 + 403V_6 - 153V_8 = 0, \quad (4)$$

where  $V_J = \langle j^2; J | \hat{V} | j^2; J \rangle$  denotes a two-body matrix element and  $J$  the angular momentum of a two-particle state  $|j^2\rangle$ . The symmetry is broken for most effective interactions in subshells with  $j \geq 9/2$  where the eigenstates would be admixtures of states with different seniorities. For a system with  $n=4$  identical fermions in a  $j=9/2$  shell, there are three  $I=4$  (and also  $I=6$ ) states, which may be constructed so that one state has seniority  $v=2$  and the other two have seniority  $v=4$ . In principle, those seniority  $v=4$  states are not uniquely defined and any linear combination of them would result in a new set of  $v=4$  states. However, it was noticed that in the  $j=9/2$  shell two special  $v=4$  states with  $I=4$  and  $6$  have good seniority for any interaction<sup>[18]</sup>. They have vanishing matrix elements with the other  $v=2$  and  $v=4$  states, irrespective of two-body interactions used. In other words, those two special  $v=4$  states are uniquely specified and are eigenstates of any two-body interaction. We denoted those special states and the  $v=4$  states orthogonal to them as  $|\alpha\rangle$  and  $|\beta\rangle$ , respectively. Detailed descriptions of the problem can be found in Refs. [13, 18–25]. Nuclear systems that can exhibit such dynamic symmetry features include the neutron-rich  $^{70-78}\text{Ni}$  isotopes<sup>[26]</sup>, the  $N=50$  and  $82$ <sup>[27]</sup> isotones in the  $0g_{9/2}$  proton subshell, neutron-rich isotopes  $^{134-140}\text{Sn}$  with in the  $1f_{7/2}$  subshell<sup>[28]</sup> as well as  $^{210-218}\text{Pb}$  in the  $1g_{9/2}$  neutron subshell<sup>[29]</sup>. In addition, certain mid-shell nuclei can also show partial seniority conversation property<sup>[30]</sup>.

We have developed an angular momentum projection technique to derive the analytic wave functions and energy expressions for those states<sup>[30]</sup>. We then proceed to type 2 states and evaluate the wave functions and eigenvalues for the two partial seniority conserved states (labelled as  $\alpha_1$ ) and the other states that are orthogonal to them in  $(9/2)^4$  configuration. The diagonal matrix elements for the  $4^+$  and  $6^+$  states read

$$\begin{aligned} E_{4+}[(9/2)^4, v=4, \alpha] &= \frac{68}{33}V_2 + V_4 + \frac{13}{15}V_6 + \frac{114}{55}V_8, \\ V_{4+}[(9/2)^4, v=4, \beta] &= \frac{47}{99}V_2 + \frac{300}{143}V_4 + \frac{1214}{495}V_6 + \frac{697}{715}V_8, \\ V_{4+}[(9/2)^4, v=2] &= \frac{3}{5}V_0 + \frac{67}{99}V_2 + \frac{746}{715}V_4 + \frac{1186}{495}V_6 + \frac{918}{715}V_8, \end{aligned} \quad (5)$$

and

$$\begin{aligned} E_{6+}[(9/2)^4, v=4, \alpha] &= \frac{19V_2}{11} + \frac{12V_4}{13} + V_6 + \frac{336V_8}{143}, \\ V_{6+}[(9/2)^4, v=4, \beta] &= \frac{61V_2}{198} + \frac{545V_4}{286} + \frac{479V_6}{198} + \frac{391V_8}{286}, \\ V_{6+}[(9/2)^4, v=2] &= \frac{3V_0}{5} + \frac{34V_2}{99} + \frac{1186V_4}{715} + \frac{658V_6}{495} + \frac{1479V_8}{715}. \end{aligned} \quad (6)$$

We have also calculated the energy expressions for other uniquely defined states in the same shell. They are given in Table 1.

Table 1 The closed energy expressions for states in the single  $j=9/2$  shell that can be uniquely specified by the total angular momentum  $I$ .  $v$  stands for the seniority number.

Confi.	$I$	$v$	Energy
$(9/2)^3$	3/2	3	$\frac{24V_4}{11} + \frac{9V_6}{11}$
	5/2	3	$\frac{5V_2}{6} + \frac{13V_4}{22} + \frac{52V_6}{33}$
	7/2	3	$\frac{52V_2}{33} + \frac{60V_4}{143} + \frac{V_6}{165} + \frac{714V_8}{715}$
	11/2	3	$\frac{17V_2}{33} + \frac{170V_4}{143} + \frac{56V_6}{165} + \frac{684V_8}{715}$
	13/2	3	$\frac{10V_2}{11} + \frac{27V_4}{143} + \frac{17V_6}{22} + \frac{323V_8}{286}$
	15/2	3	$\frac{57V_4}{143} + \frac{21V_6}{11} + \frac{9V_8}{130}$
$(9/2)^4$	3	4	$\frac{123V_4}{143} + \frac{57V_6}{110} + \frac{209V_8}{130}$
	5	4	$\frac{4V_2}{11} + \frac{327V_4}{143} + \frac{29V_6}{11} + \frac{102V_8}{143}$
	7	4	$V_2 + \frac{228V_4}{143} + \frac{101V_6}{55} + \frac{102V_8}{65}$
	9	4	$\frac{79V_2}{66} + \frac{313V_4}{286} + \frac{463V_6}{330} + \frac{3297V_8}{1430}$
	10	4	$\frac{V_2}{6} + \frac{381V_4}{286} + \frac{701V_6}{330} + \frac{309V_8}{130}$
	12	4	$\frac{23V_2}{33} + \frac{98V_4}{143} + \frac{233V_6}{165} + \frac{2292V_8}{715}$
	12	4	$\frac{75V_4}{143} + \frac{93V_6}{55} + \frac{246V_8}{65}$
$(9/2)^5$	1/2	5	$\frac{19V_2}{11} + \frac{30V_4}{11} + \frac{169V_6}{55} + \frac{136V_8}{55}$
	3/2	3	$\frac{2V_0}{5} + \frac{25V_2}{22} + \frac{2373V_4}{1430} + \frac{284V_6}{55} + \frac{1173V_8}{715}$
	19/2	5	$\frac{8V_2}{11} + \frac{291V_4}{143} + \frac{349V_6}{110} + \frac{5813V_8}{1430}$
	21/2	3	$\frac{2V_0}{5} + \frac{49V_2}{66} + \frac{1983V_4}{1430} + \frac{859V_6}{330} + \frac{6961V_8}{1430}$

The existence of partial conservation of seniority in  $j=9/2$  shells plays an essential role in our understanding of the electric quadrupole transitions of and the existence of isomeric states in the nuclei involved<sup>[31]</sup>. As can be seen from Fig. 1 in that paper, the transition scheme can be significantly different depending on the relative positions of the  $4^+$  and  $6^+$  states. If they are lower than the  $v=2$  states, a collectivity-like strong inner-band E2 transition can be expected. In addition, the half life of the  $8^+$  state also depend strongly on the position and the structure of the  $6^+$  states. The existence of the uniquely defined  $v=4, \alpha$  states makes it possible to understand the  $B(E2; 8_1^+ \rightarrow 6_1^+)$  value and its strong suppression in  $^{94}\text{Ru}$  from a very simple perspective.

Another fundamental question is how the unique states mentioned above, which are defined for single- $j$  systems, are influenced by configuration mixing from other neighbouring subshells. This is important also by considering the fact that the lightest semi-magic



nuclei that involve a  $j=9/2$  orbital, including the Ni isotopes between  $N=40$  and 50 and  $N=50$  isotones between  $Z=40$  and 50, are expected to be dominated by the coupling within the  $0g_{9/2}$  shell but may also contain non-negligible contribution from other neighbouring orbitals (including  $1p_{1/2}, 1p_{3/2}, 0f_{5/2}$ ). We have shown that a sharp transition from pure seniority coupling to significant mixing between the  $v=2$  and  $v=4, \alpha$  states may be induced by the cross-orbital non-diagonal interaction matrix elements<sup>[31]</sup>, as can also be seen in Fig. 2. Such strong mixture is essential to explain the observed E2 transition properties of  $N=50$  isotones  $^{96}\text{Pd}$  and  $^{94}\text{Ru}$ . In particular, the  $B(\text{E}2; 4_1^+ \rightarrow 2_1^+)$  value for  $^{96}\text{Pd}$  was measured to be significantly suppressed by roughly a factor of seven in comparison with that predicted by a seniority-conserved interaction. This feature can not be explained without considering the symmetry breaking effect from the cross-shell matrix elements.

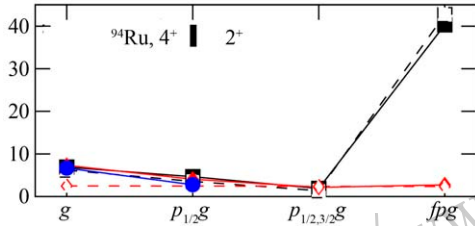


Fig. 2 (color online)  $4_{v'=2}^+ \rightarrow 2_{v'=2}^+$  E2 transition strengths (divided by the square of the effective charge, in  $\text{fm}^4$ ) for  $^{94}\text{Ru}$  calculated in different model spaces with effective interactions from Refs. [32] (square), [33] (diamond) and [34] (circle). The open symbols correspond to the calculations for  $^{72,74}\text{Ni}$ .

We have also studied seniority coupling scheme in multi-shells which may be found in Refs. [31, 35–36]. One can also derive the exact solution of the pairing Hamiltonian by diagonalizing the matrix spanned by the seniority  $v=0$ , spin  $I=0$  states which represent only a tiny part of the total wave function. This is applied in Ref. [4, 37–38]. We have also done pair-truncated shell-model calculations with collective pairs as building blocks in Refs. [6, 39–40] for both the standard shell model and continuum shell model in the complex energy plane.

#### 4 Nuclei above $^{100}\text{Sn}$

There have been significant experimental<sup>[41–52]</sup> and theoretical<sup>[3, 53–60]</sup> efforts in studying the spectroscopy and transition properties of  $N \sim Z$  nuclei just above the presumed doubly magic nucleus  $^{100}\text{Sn}$ . Several unexpected phenomena have been observed: Unusually large  $B(\text{E}2; 2_1^+ \rightarrow 0_1^+)$  values are observed neutron deficient semi-magic Sn isotopes; Whereas the

low-lying spectra in Te isotopes show typical vibration, the available E2 transition strengths along the yrast line in  $^{114,120-124}\text{Te}$  show a rotational-like behaviour, which can not be explained by collective models<sup>[1, 61]</sup>. An enhanced interplay between neutrons and protons is expected in the  $^{100}\text{Sn}$  region since the protons and neutrons partially occupy the same quantum orbitals near the Fermi level<sup>[62–65]</sup>; There has also been a long effort searching for superallowed alpha decays from those  $N \sim Z$  isotopes<sup>[66–67]</sup>; another intriguing phenomenon is the nearly constant behaviour of the energies of the  $2^+$  and  $4^+$  states in Te and Xe isotopes and their ratios when approaching  $N=50$ , in contrast to the decreasing behaviour when approaching  $N=82$ <sup>[63]</sup>, which may be related to an enhanced neutron-proton correlation. In relation to that, it may be interesting to mention that there has been a long quest for the possible existence of np pairing in  $N \sim Z$  nuclei (see, recent discussions in Refs. [39, 68–71]).

The study of transition rates in isotopic chains just above  $Z=50$  may provide further information on the role of core excitations<sup>[72–73]</sup>. It was argued that  $^{100}\text{Sn}$  may be a soft core in analogy to the soft  $N=Z=28$  core  $^{56}\text{Ni}$ . It seems such a possibility can be ruled out based on indirect information from recent measurements in this region<sup>[3, 48, 72–74]</sup>. The asymmetric electric quadrupole (E2) transition shape in Sn isotopes is suggested to be induced by the Pauli blocking effect<sup>[3]</sup>.

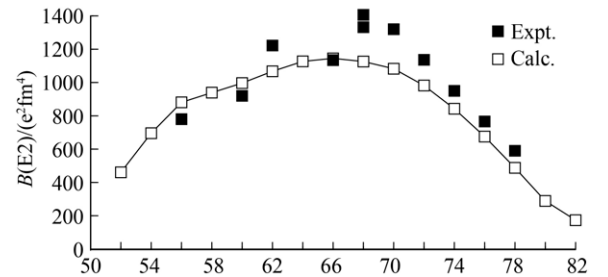


Fig. 3 (color online) Systematics of the E2 transition strengths in Te isotopes.

The limited number of valence protons and neutrons are not expected to induce any significant quadrupole correlation in this region<sup>[63, 75–77]</sup>. A systematic study on the E2 transition in Te isotopes is done in Ref. [73]. In Fig. 3 we plotted the comparison between the experimental and calculated  $B(\text{E}2)$  values as a function of neutron number. The low-lying collective excitations of Te isotopes were discussed in terms of quadrupole vibrations<sup>[63, 78]</sup> in relation to the fact that the even-even isotopes between  $N=56$  and 70 show regular equally-spaced yrast spectra (*c.f.*, Fig. 1 in Ref. [63]). If that is the case, the Te isotopes will provide an ideal ground to explore the na-

ture of the elusive nuclear vibration and the residual interactions that leading to that collectivity. However, their exotic transition property mentioned above indicates that the Te isotopes may not be dominated by vibration but by other kinds of correlation. Still, compared to tin, the experimental information is less abundant in the isotopic chain of tellurium where little was known experimentally below the neutron midshell until recently<sup>[73, 79]</sup>. Much more work is needed in order to map out the ordering and nature of single-particle states and two-body effective interactions in the region. We have done systematic calculations on the E2 transition properties of Te isotopes in Ref. [80]. The calculations reproduce well the excitation energies of the low-lying states as well as the regular and vibrational-like behaviour of the yrast spectra of <sup>108–130</sup>Te. The shell-model calculations for mid-shell Te isotopes, in particular <sup>118</sup>Te, are quite sensitive to the filling of both the proton and neutron  $h_{11/2}$  subshells. Both the proton and neutron transition matrix elements can be significantly enhanced when one goes from a small model space calculation with restricted number of particles in  $h_{11/2}$  to the full shell-model calculation. In particular, the calculations reproduced reasonably well the nearly constant behaviour of the  $B(E2)$  values of <sup>114</sup>Te and <sup>120–124</sup>Te along the yrast line. The anomalous constant behaviour is related to the competition between the seniority coupling and the neutron-proton correlations. On the other hand, a squeezed gap between the  $6_1^+$  and  $4_1^+$  states is seen in Te isotopes when approaching  $N=82$ , resulting in seniority-like spectra. A further experiment is done to study the angular momentum dependence of the E2 transition strengths in <sup>112</sup>Te<sup>[81]</sup>. It shows a similar but more ‘vibrational’-like behaviour. Potential-Energy Surface calculations indicate that those nuclei may also be understood from a soft rotor point of view. We have done further calculations on the E2 transitions of Cd isotopes (with two proton holes instead of particles within  $Z=50$  closure). The results will be published soon.

One puzzle we still do not understand is that the ratio  $B(E2, 4_1^+ \rightarrow 2_1^+)/B(E2, 2_1^+ \rightarrow 0_1^+)$  for <sup>114</sup>Te is actually measured to be even slightly smaller than one. The ratio is calculated to be  $B(E2, 4_1^+ \rightarrow 2_1^+)/B(E2, 2_1^+ \rightarrow 0_1^+) = 1.38$  which, on the other hand, is close to the prediction for a rotor. In Ref. [61], the ratios  $B(E2, 4_1^+ \rightarrow 2_1^+)/B(E2, 2_1^+ \rightarrow 0_1^+)$  for isotopes <sup>120–124</sup>Te are measured to be 1.640, 1.500 and 1.162, respectively. The ratios calculated from the shell model  $B(E2)$  values are 1.322, 1.299, and 1.301, respectively, for above three nuclei, which agree reasonably with experimental data. In a recent paper, we have also measured the  $B_{4/2}$  ratio for <sup>112</sup>Te<sup>[79]</sup>, which is also larger than

one. In addition to the large-scale shell model, we have done potential energy surface calculations on <sup>112,144</sup>Te which indicates that the former can be more gamma soft than the latter nucleus.

Another interesting example we studied is the proton-unbound nucleus <sup>109</sup>I<sup>[82]</sup> for which the level structure and E2 transition properties are very similar to those of <sup>108</sup>Te<sup>[72]</sup> and <sup>109</sup>Te<sup>[83]</sup>, indicating that the odd proton in <sup>109</sup>I is weakly coupled to the <sup>108</sup>Te daughter nucleus like a spectator.

We have also studied the structure and electromagnetic transition properties of low-lying non-yrast states in Sn, Te and Xe isotopes, which may help us understanding the underlying dynamic symmetry. In Figs. 4 and 5 we plotted the calculated excitation energies of the second and third  $0^+$  states in Te and Xe isotopes and compared with available experimental data. A good agreement is seen. As for the neutron deficient Pb isotopes, the calculation can produce well the excitation energies of excited  $0^+$  states in nuclei close to <sup>208</sup>Pb but overestimate the energies of those states when approaching mid-shell  $N=104$ .

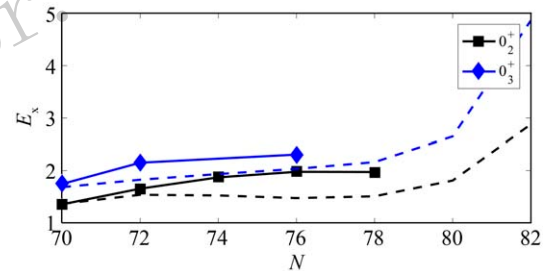


Fig. 4 (color online) Systematics the experimental (solid line) and calculated (dashed line) excitation energies of the excited  $0^+$  states in Te isotopes.

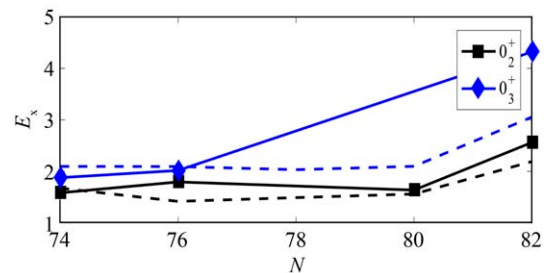


Fig. 5 (color online) Systematics the experimental (solid line) and calculated (dashed line) excitation energies of the excited  $0^+$  states in Xe isotopes.

## 5 Neutron-deficient transitional nuclei around $N=90$

There have been extensive studies in recent years concerning the possible existence of the so-called quantum phase transition in finite many-body systems like nuclei, in particular those around neutron number  $N=60$  and  $N=90$ . Most studies focus on the system-

atics of the spectra and binding energies of those nuclei. We have measured the lifetimes of the first excited  $2^+$  and  $4^+$  states in the neutron-deficient nuclide  $^{172}\text{Pt}$  at JYFL, University of Jyväskylä, Finland using recoil-distance Doppler shift and recoil-decay tagging techniques<sup>[84]</sup>. A striking feature we found is that the ratio  $B(E2; 4_1^+ \rightarrow 2_1^+)/B(E2; 2_1^+ \rightarrow g.s.)=0.55(19)$  is unusually low. In addition, a few other neutron-deficient W, Os, and Pt nuclei in this region feature the same effect<sup>[85]</sup>. The phenomenon is highly unexpected for these nuclei which are not situated near closed shells. Such feature cannot be explained by the geometrical collective model or algebraic interacting boson model. A system governed by seniority symmetry is the only known framework for which such an effect may naturally occur, We thus speculate that a quantum phase transition from a seniority conserving structure to a collective regime may have happened in this region as the neutron number increases.

We have done several large-scale shell model calculations with realistic nucleon-nucleon interactions for Pt, Os and W isotopes between  $N=82$  and  $94$  by considering either  $^{132}\text{Sn}$  or  $^{146}\text{Gd}$  as the inert cores. All neutron levels between  $N=82$  and  $126$  are included. The cross-shell neutron-proton interactions are evaluated from the charge-dependent Bonn nucleon-nucleon potential with slight modifications to reproduce better the properties of  $N=84$  isotones<sup>[86]</sup>. The large-scale calculations reproduce reasonably well the excitation energies as well as the  $B(E2; 2_1^+ \rightarrow g.s.)$  values for those nuclei. The calculation also agrees with the tentative spin-parity assignment for  $^{171}\text{Pt}$ . However, as shown in Fig. 6, the calculations with our standard neutron-proton interaction predict larger values for  $B(E2; 4_1^+ \rightarrow 2_1^+)$ .

The orbitals that are most relevant for those nuclei include the proton  $h_{11/2}$  and neutron  $g_{9/2}$ ,  $f_{7/2}$  and  $i_{13/2}$ . The calculated ratio between  $B(E2; 4_1^+ \rightarrow 2_1^+)$  and  $B(E2; 2_1^+ \rightarrow g.s.)$  is sensitive to the relative positions between the neutron  $g_{9/2}$ ,  $f_{7/2}$  and  $i_{13/2}$  orbitals and to the quadrupole-quadrupole channel of the neutron-proton interaction. The neutron  $g_{9/2}$ ,  $f_{7/2}$  orbitals are well separated when approaching  $N=82$ . However, our large-scale shell model calculations indicate that the neutron  $h_{9/2}$ ,  $f_{7/2}$  subshell are indeed strongly mixed and nearly degenerate as a result of the attractive neutron-proton  $\nu h_{9/2} - \pi h_{11/2}$  monopole interaction. The mixture of the two orbitals leads to a strongly enhanced  $B(E2; 4_1^+ \rightarrow 2_1^+)$  in the calculation. In this scenario it is also possible to explain the observed  $2^+$  and  $4^+$  excitation energies and the observed absolute transition strengths, which are tens of Weisskopf units. The small  $B_{4/2}$  value requires

the neutron-proton quadrupole-quadrupole interaction strength for these nuclei to be weaker than for the standard nucleon-nucleon interaction used in other mass regions. The ratio  $B_{4/2}$  indeed reduces to around 0.6 if we only consider wither proton-hole or neutron degrees of freedom by suppressing the neutron-proton interaction.

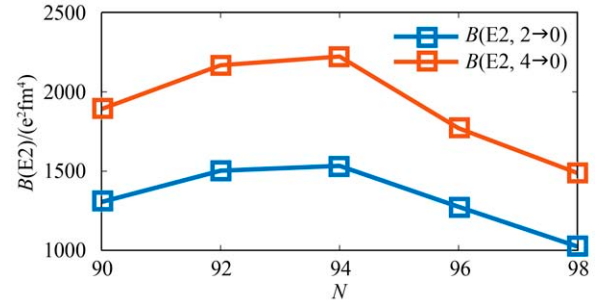


Fig. 6 (color online) Calculated  $B(E2)$  values for the transitions from  $4^+$  and  $2^+$  states in Pt isotopes as a function of neutron number.

We have also calculated the higher-lying states in  $^{172}\text{Pt}$  and compared with the data we obtained recently. A quite good overall agreement is obtained except the  $3^-$  state which is expected to show strong octupole vibration.

## 6 Summary and future work

To summarize, in this work we present an overview on our recent experimental and theoretical studies of the half-lives of the lowest-lying states in certain transitional nuclei, in particular those show 'regular' nuclear spectra but exotic electromagnetic transition properties. We analysed the electric quadrupole transition properties of semi-magic nuclei with four particles or four holes in the  $g_{9/2}$  orbital from a partial seniority conservation perspective. This is related to the existence of uniquely defined  $\nu=4$  states which, for systems within a  $j=9/2$  subshell, do not mix with other states. The diminishing  $B(E2; 8_1^+ \rightarrow 6_1^+)$  in  $^{94}\text{Ru}$  can be mostly understood as the cancellation between few terms induced by the seniority-non-conserving interaction. Moreover, the cross-orbital interaction matrix elements can induce significant mixture between the  $\nu=2$  and the unique  $\alpha$  states. As a result, a sharp phase transition can be expected in nuclei like  $^{96}\text{Pd}$  and  $^{94}\text{Ru}$ .

I also presented briefly our recent works on the configuration interaction shell model calculations of the spectroscopy and transition properties of intermediate-mass and heavy nuclei. I started by introducing the basic framework of the nuclear shell model and the monopole channel of the effective Hamiltonian. A simple truncation scheme can be established by con-

sidering configurations with lowest monopole energies, which I refer to as the importance-truncation approach. Large scale calculations have been carried out to study the spectroscopic and transition properties of nuclei around  $^{100}\text{Sn}$  and  $^{208}\text{Pb}$  that cannot be reached by standard shell model calculations.

The yrast spectra of Te isotopes show a vibrational-like equally spaced pattern but the few known E2 transitions show anomalous rotational-like behaviour, which cannot be reproduced by collective models. This feature is well reproduced in the theory. The Hamiltonian works well also for Sb, I and Xe isotopes but show relatively larger deviations from experimental data for selected other nuclei including Cs and Lu isotopes. We are also optimizing the  $T=0$  channel of the effective interaction. In addition, we are extending the model space to include orbitals between the  $N=Z=50$  shell closure as well as neutron orbitals above  $N=82$  in order to study the structure of neutron-rich Cd isotopes.

We also studied the spectra and E2 transition properties of transitional nuclei around  $N=90$ , in particular  $^{172}\text{Pt}$ . An unusually low  $B_{4/2}$  value of 0.55(19) is observed, which can be explained by theory only if we assume the onset of strong seniority coupling. This observation might reveal a pattern indicating a transition from a seniority-conserving structure to a collective regime.

One can state that the coupling of 'a few' particles can already lead to rich physics, which can provide a critical test of the nuclear shell model and our understanding of the underlying nuclear interaction.

**Acknowledgement** The computations were performed on resources provided by the Swedish National Infrastructure for Computing (SNIC) at PDC, KTH, Stockholm and NSC, Linköping. Collaboration with R. Liotta, R. Wyss, T. Bäck, A. Johnson, A. Nyberg, B. Cederwall (KTH, Stockholm) Liyuan Jia, Guanjian Fu, YiYuan Cheng (Shanghai), Y.B. Qian (Nanjing) and X. Guan (Dalian) is acknowledged. I would also like to thank F. Pan and Y. Zhang for their hospitality during my stay in Liao-Ning Normal University, Dalian.

## References:

- [1] MÖLLER O, WARR N, JOLIE J, *et al.* Phys Rev C, 2005, **71**: 064324.
- [2] ÇAKIRLI R B, CASTEN R F, JOLIE J, *et al.* Phys Rev C, 2004, **70**: 047302.
- [3] BACK T, QI C, CEDERWALL B, *et al.* Phys Rev C, 2013, **87**: 031306.
- [4] XU Z X, QI C. Phys Lett B, 2013, **724**: 247.
- [5] JIAO L F, SUN Z H, XU Z X, *et al.* Phys Rev C, 2014, **90**: 024306.
- [6] QI C, JIA L Y, FU G J. Phys Rev C, 2016, **94**: 014312.
- [7] QI C. Journal of Physics: Conference Series, 2016, **742**: 012030.
- [8] ANDREYEV A N. Phys Rev Lett, 2013, **110**: 242502.
- [9] QI C, ANDREYEV A N, HUYSE M, *et al.* Phys Lett B, 2014, **734**: 203.
- [10] WANG F, SUN B H, LIU Z, *et al.* Phys Rev C, 2017, **96**: 064307.
- [11] WANG F. Phys Lett B, 2017, **770**: 83.
- [12] TALMI I. Simple Models of Complex Nuclei: The Shell Model and Interacting Boson Model[M]. Amsterdam: Harwood Academic Publishers, 1993.
- [13] VAN ISACKER P, HEINZE S. Annals of Physics, 2014, **349**: 73
- [14] QI C. Phys Rev C, 2010, **81**, 034318.
- [15] ROWE D J, ROSENSTEEL G. Phys Rev Lett, 2001, **87**: 172501.
- [16] ROSENSTEEL G, ROWE D J. Phys Rev C, 2003, **67**: 014303.
- [17] QI C, WANG X B, XU Z X, *et al.* Phys Rev C, 2010, **82**: 014304.
- [18] ESCUDEROS A, ZAMICK L. Phys Rev C, 2006, **73**: 044302.
- [19] VAN ISACKER P. Nuclear Physics News, 2014, **24**: 23.
- [20] ZAMICK L. Phys Rev C, 2007, **75**: 064305.
- [21] QI C, XU Z X, LIOTTA R J. Nucl Phys A, 2012, **884**: 21.
- [22] VAN ISACKER P, HEINZE S. Phys Rev Lett, 2008, **100**: 052501.
- [23] QI C. Phys Rev C, 2011, **83**: 014307.
- [24] LEVIATAN A. Prog Part Nucl Phys, 2011, **66**: 93.
- [25] VAN ISACKER P. Int J Mod Phys E, 2011, **20**: 191.
- [26] MORALES A I. Phys Rev C, 2016, **93**: 034328.
- [27] WATANABE H. Phys Rev Lett, 2013, 111: 152501.
- [28] SIMPSON G S. Phys Rev Lett, 2014, **113**: 132502.
- [29] GOTTARDO A. Phys Rev Lett, 2012, **109**: 162502.
- [30] QIAN Y B, QI C. Phys Rev C, 2018, **98**: 061303.
- [31] QI C. Phys Lett B, 2017, **773**: 616.
- [32] HONMA M, OTSUKA T, MIZUSAKI T, *et al.* Phys Rev C, 2009, **80**: 064323.
- [33] LISETSKIY A F, BROWN B A, HOROI M, *et al.* Phys Rev C, 2004, **70**: 044314.
- [34] BLOMQVIST J, RYDSTRÖM L. Physica Scripta, 1985, **31**: 31.
- [35] QI C. Phys Lett B, 2012, **717**: 436.
- [36] JIA L Y, QI C. Phys Rev C, 2016, **94**: 044312.
- [37] QI C, CHEN T. Phys Rev C, 2015, **92**: 051304.
- [38] CHANGIZI S, QI C, WYSS R. Nucl Phys A, 2015, **940**: 210.
- [39] XU Z X, QI C, BLOMQVIST J, *et al.* Nucl Phys A, 2012, **877**: 51.
- [40] JIANG H, QI C, LEI Y, *et al.* Phys Rev C, 2013, **88**: 044332.
- [41] BANU A. Phys Rev C, 2005, **72**: 061305.
- [42] CORSI A. Phys Lett B, 2015, **743**: 451.
- [43] CEDERKÄLL J. Phys Rev Lett, 2007, **98**: 172501.



- [44] CERIZZA G. Phys Rev C, 2016, **93**: 021601.  
 [45] EKSTRÖM A. Phys Rev Lett, 2008, **101**: 012502.  
 [46] DOORNENBAL P. Phys Rev C, 2014, **90**: 061302.  
 [47] JUNGCLAUS A. Phys Lett B, 2011, **695**: 110.  
 [48] GUASTALLA G. Phys Rev Lett, 2013, **110**: 172501.  
 [49] ALLMOND J. M. Phys Rev C, 2015, **92**: 041303  
 [50] SPIEKER M. Phys Lett B, 2016, **752**: 102.  
 [51] PELLEGGRI L. Phys Rev C, 2015, **92**: 014330.  
 [52] FAESTERMANN T, GORSKA M, GRAWE H. Prog Part Nucl Phys, 2013, **69**: 85.  
 [53] ANSARI A, RING P. Phys Lett B, 2007, **649**: 128.  
 [54] LO IUDICE N, STOYANOV C., TARPANOV D. Phys Rev C, 2011, **84**: 044314.  
 [55] MORALES I O, VAN ISACKER P, TALMI I. Phys Lett B, 2011, **703**: 606.  
 [56] JIANG H, LEI Y, QI C, *et al.* Phys Rev C, 2014, **89**: 014320.  
 [57] JIANG H, LEI Y, FU G J, *et al.* Phys Rev C, 2012, **86**: 054304.  
 [58] CORAGGIO L, COVELLO A, GARGANO A, *et al.* Phys Rev C, 2015, **91**: 041301.  
 [59] ENGELAND T, HJORTH-JENSEN M, KARTAMYSHEV M, *et al.* Nucl Phys A, 2014, **928**: 51.  
 [60] QI C, XU Z X. Phys Rev C, 2012, **86**: 044323.  
 [61] SAXENA M. Phys Rev C, 2014, **90**: 024316.  
 [62] HADINIA B. Phys Rev C, 2004, **70**: 031302  
 [63] HADINIA B. Phys Rev C, 2005, **72**: 041303.  
 [64] SANDZELIUS M. Phys Rev Lett, 2007, **99**: 022501.  
 [65] DELION D S, WYSS R, LIOTTA R J, *et al.* Phys Rev C, 2010, **82**: 024307.  
 [66] SEWERYNIAK D. Phys Rev C, 2006, **73**: 061301.  
 [67] LIDDICK S N. Phys Rev Lett, 2006, **97**: 082501.  
 [68] CEDERWALL B. Nature, 2011, **469**: 68.  
 [69] FRAUENDORF S, MACCHIAVELLI A. Prog Part Nucl Phys, 2014, **78**: 24.  
 [70] QI C, BLOMQUIST J, BÄCK T, *et al.* Phys Rev C, 2011, **84**: 021301.  
 [71] QI C, WYSS R. Physica Scripta, 2016, **91**: 013009.  
 [72] BÄCK T. Phys Rev C, 2011, **84**: 041306.  
 [73] DONCEL M. Phys Rev C, 2015, **91**: 061304.  
 [74] HINKE C B, BÖHMER M, BOUTACHKOV P, *et al.* Nature, 2012, **486**: 341.  
 [75] CAURIER E, NOWACKI F, POVES A, *et al.* Phys Rev C, 2010, **82**: 064304.  
 [76] WU Z Y, QI C, WYSS R, *et al.* Phys Rev C, 2015, **92**: 024306.  
 [77] COELLO PÉREZ E A, PAPENBROCK T. Phys Rev C, 2015, **92**: 064309.  
 [78] DOMBRÁDI Z. Phys Rev C, 1995, **51**: 2394.  
 [79] DONCEL M. Phys Rev C, 2017, **95**: 044321.  
 [80] QI C. Phys Rev C, 2016, **94**: 034310.  
 [81] DONCEL M, BÄCK T, QI C, *et al.* Phys Rev C, 2017, **96**: 051304.  
 [82] PROCTER M G. Phys Lett B, 2011, **704**: 118.  
 [83] PROCTER M G. Phys Rev C, 2012, **86**: 034308.  
 [84] CEDERWALL B, DONCEL M, AKTAS O, *et al.* Phys Rev Lett, 2018, **121**: 022502.  
 [85] GRAHN T. Phys Rev C, 2016, **94**: 044327.  
 [86] CARROLL R J. Phys Rev C, 2016, **94**: 064311.

## 中重核中单粒子与集体运动的竞争效应

亓冲<sup>1)</sup>

(瑞典皇家工学院物理系, 瑞典 斯德哥尔摩 100691)

**摘要:** 从原子核的电四极跃迁强度 $B(E2)$ 中可以提取出原子核集体性和单粒子性质竞争的重要信息, 其中一个重要的观测量是 $B(E2; 4_1^+ \rightarrow 2_1^+)/B(E2; 2_1^+ \rightarrow g.s.)$ 的比值( $B_{4/2}$ )。  $B_{4/2}$  一般要大于1, 而且对于原子核转动和振动, 我们应有 $B_{4/2}=1.4$ 和2.0, 但球形半满壳核一般会有不一样的性质。这些核的性质主要受对关联效应影响。介绍了几种超出我们一般认识的奇特衰变性质。Te同位素的基态带有鲜明的振动特性, 但 $^{114}\text{Te}$ 的E2跃迁性质却更符合转动性。这些性质可以通过大规模壳模型计算来描述。对于填充 $j=9/2$ 轨道的半满壳核, 它们的 $4^+$ 和 $6^+$ 显示出很强的辛若数部分守恒性质。这种奇特的部分守恒可以被解析证明。而且我们的计算表明辛若数部分守恒对相关的E2跃迁影响很大。对于 $N=90$ 附近具有量子相变行为的核素, 其 $B_{4/2}$ 也会表现出相似的奇异特性。

**关键词:** 电磁跃迁; 壳模型; 辛若数; 集体性

收稿日期: 2018-10-18

基金项目: 瑞典研究理事会项目(621-2012-3805, 621-2013-4323); Göran Gustafsson基金杰出青年项目

1) E-mail: chongq@kth.se; chong.kth@gmail.com.